Modeling the effects of small turbulent scales on the drag force for particles below and above the Kolmogorov scale

Mikhael Gorokhovski
Laboratoire de Mécanique des Fluide et d'Acoustique (LMFA)-Université de Lyon, CNRS-ECL-INSA-UCBL, Lyon, France

Rémi Zamansky
Institut de Mécanique des Fluides de Toulouse, IMFT, Université de Toulouse, CNRS-Toulouse, France

(Received 18 September 2017; published 9 March 2018)

Consistently with observations from recent experiments and DNS, we focus on the effects of strong velocity increments at small spatial scales for the simulation of the drag force on particles in high Reynolds number flows. In this paper, we decompose the instantaneous particle acceleration in its systematic and residual parts. The first part is given by the steady-drag force obtained from the large-scale energy-containing motions, explicitly resolved by the simulation, while the second denotes the random contribution due to small unresolved turbulent scales. This is in contrast with standard drag models in which the turbulent microstructures advected by the large-scale eddies are deemed to be filtered by the particle inertia. In our paper, the residual term is introduced as the particle acceleration conditionally averaged on the instantaneous dissipation rate along the particle path. The latter is modeled from a log-normal stochastic process with locally defined parameters obtained from the resolved field. The residual term is supplemented by an orientation model which is given by a random walk on the unit sphere. We propose specific models for particles with diameter smaller and larger size than the Kolmogorov scale. In the case of the small particles, the model is assessed by comparison with direct numerical simulation (DNS). Results showed that by introducing this modeling, the particle acceleration statistics from DNS is predicted fairly well, in contrast with the standard LES approach. For the particles bigger than the Kolmogorov scale, we propose a fluctuating particle response time, based on an eddy viscosity estimated at the particle scale. This model gives stretched tails of the particle acceleration distribution and dependence of its variance consistent with experiments.

DOI: 10.1103/PhysRevFluids.3.034602

I. INTRODUCTION

High Reynolds number turbulent flows laden by heavy particles can be observed in many natural phenomena and industrial applications. For the characterization and the control of such flows, a clear understanding of how the particles respond to the carrier flow is essential. The difficulty is that the computation of the instantaneous forces on a particle of finite size requires the accurate resolution of all turbulent scales involved in the motion of this particle, and with the present computer technology, this is still effectively impossible for most problems of practical importance. It is a common practice to consider particles as material inertial points, and to use unresolved descriptions, known as large eddy simulations (LES) to compute the carrier flow. In the LES approaches, the large-scale velocity field $\overline{u}_f$ is resolved explicitly from spatially filtered equations while the small-scale motions can be accounted for through a turbulent viscosity ν_Δ that ensures a correct energy flux below the resolved scale, ε_Δ [1,2]. When particles are small and much denser than the carrier phase, their acceleration

is primarily given by the drag force [3,4], and the particles respond to the fluid solicitation with a time lag τ_p. Because of the response time of the particles acting as a temporal filtering of the high frequency fluid velocity fluctuations, it is usually assumed that the turbulent microstructure, advected by the large-scale eddies, does not influence the particle motion. Therefore, it is considered that the dynamics of the inertial particles mainly result from interactions with the energy-containing large-scale motions, resolved by the LES:

$$\mathbf{a}_p = \frac{d\mathbf{u}_p}{dt} = -\frac{\mathbf{u}_p - \overline{\mathbf{u}}_{f(\mathbf{x}=\mathbf{x}_p)}}{\tau_p}, \tag{1}$$

where $\mathbf{a}_p$ is the particle acceleration, $\mathbf{u}_p$ is the particle velocity, and $\mathbf{x}_p$ is the particle position. For a small heavy spherical non-rotating particle, subjected to a velocity field that is uniform and stationary at its scale, the response time is $\tau_p = \rho_p/\rho_f\, d_p^2/18\nu$, with d_p, ν, and ρ_p/ρ_f being respectively the particle diameter, the fluid viscosity and the particle to fluid density ratio.

However, measurements in high Reynolds flows showed that particles present highly non-Gaussian acceleration probability density function (PDF) [5–11]. The broad probability tails of high acceleration events are related to the highly non-Gaussian PDF of the velocity increments at small scales. Those scales are associated typically with the large fluctuations of the dissipation rate of turbulent kinetic energy ε [12–15]. Consequently, since the small scales are smoothed out from the evolution of the filtered velocity field $\overline{u}_f$, Eq. (1) needs to be extended. Similar conclusions can also be found in Ref. [16]. The importance of the small scales of the flow, and particularly the fluctuations of the viscous dissipation of turbulent energy, was already emphasized in Ref. [17]. Applying the formula from Ref. [18]: $\langle (u_p - u_f)^2 \rangle = \int_0^\infty d\omega E(\omega) \frac{(\omega\tau_p)^2}{1+(\omega\tau_p)^2}$, where the brackets denote the averaged along the particle path, ω is the frequency, and taking the spectral density of the velocity fluctuations along the particle trajectory as $E(\omega) \sim \langle\varepsilon\rangle/\omega^2$ [19], the following expression was given:

$$\langle (\mathbf{u}_f - \mathbf{u}_p)^2 \rangle \sim \langle\varepsilon\rangle\tau_p. \tag{2}$$

Here it is assumed that $\tau_L \gg \tau_p \gg \tau_\eta$ with τ_L and τ_η the integral time scale and the Kolmogorov time scale, respectively. We conclude from this expression that the viscous dissipation appears as a key parameters for the modeling of the drag force. Moreover, according to the refined Kolmogorov hypotheses, it is expected that the particle dynamics mainly stem from the large fluctuations of the dissipation rate. Additionally, one can see from Eq. (2), in case of statistical stationarity, $\frac{d}{dt}\langle \mathbf{u}_p^2 \rangle = 0$, that the correlation between the fluid velocity and the particle acceleration is given by $\langle \mathbf{u}_f \mathbf{a}_p \rangle = \langle\varepsilon\rangle$, which implies that the main contribution to this correlation is also dependent on the strong fluctuations of the viscous dissipation. This motivates us to develop models in which the particle response to the large fluctuations, present at the residual scales, is taken into account. To this end, later on in this paper, we refine Eq. (2) to account for the Stokes and Reynolds numbers dependency, and introducing as well the intermittency effects along the particle path.

Along with particles below the Kolmogorov scale, we also consider particles with diameter above the Kolmogorov scale, $d_p > \eta$. For a large particle, despite its important inertia, the turbulent fluctuations of the fluid at the scale of the particle is the source of an additional agitation for the particle. It was underlined in Ref. [10] that the turbulent time scale of the flow at the size of the particle should play a primary role in the particle dynamics. As observed in the experiments of Refs. [5,8,11,20,21], even for large particles, the acceleration present non-Gaussian fluctuations with a variance decreasing as $d_p^{-2/3}$. In the numerical simulations of dispersed-phase flows of Refs. [22,23] the finite-size effects are accounted by averaging the fluid quantities around the particle introducing a so-called Faxén correction term. The approach proposed here is different. Assuming that the particle diameter remains smaller than the coarse mesh resolution, $d_p < \Delta$, the particle is still viewed as a point-particle. Further, to account for the turbulent fluctuations at the scale of the particle, we introduced a stochastic turbulent particle response time based on the local velocity fluctuations at the scale of the particle diameter.

As discussed above, in the framework of LES, it appears necessary to account for the fluctuations both in the estimation of the fluid-particle relative velocity and for the inhomogeneity of flow fields at the scale of the particle (for particles larger than the dissipative scale of the flow η). The general question addressed in this paper is: how to account for the full spectrum of the flow velocity fluctuations in the particles-turbulence interaction? Various strategies have been tested to address this issue (see Ref. [24] for a comprehensive review). In most of these approaches, the unresolved scales of the Lagrangian dynamics are reproduced using stochastic models for the flow on subgrid scales [25–35]. Note also the approach of Ref. [36] in which a determinist surrogate of the fluid velocity at the particle position is obtained from the filtered velocity field.

In difference with these approaches, we propose in this paper to replace Eq. (1), by the decomposition of the instantaneous particle acceleration into a large-scale contribution and a random contribution:

$$\mathbf{a}_p = \underbrace{\widehat{\mathbf{a}}_p}_{\substack{\text{large scale}\\ \text{contribution}}} + \underbrace{\langle \mathbf{a}_p^* | \varepsilon_f \rangle}_{\substack{\text{unresolved scale}\\ \text{contribution}}} . \tag{3}$$

The first term represents the response to the large-scale sweeps governed by the resolved fluid velocity field and the second one, the residual acceleration, accounts for fluctuations at unresolved scales. Following the refined Kolmogorov hypothesis, the fluctuations at the unresolved scales are primarily attributed to the fluctuation of the energy transfer rate towards smaller scales and the residual acceleration is represented as conditionally averaged on the local value of the energy transfer rate "seen" along the particle path. This energy flux has to be also modeled since its wide fluctuations cannot be resolved from the filtered velocity field. In this paper, we compute a surrogate of the local dissipation rate by a log-normal stochastic process which primarily depends on the local coarse-grained dissipation rate computed from the LES mesh. The further modeling of the amplitude of the random term is based on the first-hand on an estimation of the particle relative velocity derived in this paper and, on the other hand, on the introduction of a fluctuating relaxation time scale for particles larger than the Kolmogorov scale. The modeling of the residual part is completed by a stochastic orientation model which includes both alignment with the large scales and return to isotropy.

The paper is organized as follows. In Sec. II, we present the numerical details of the LES used to obtain the filtered fluid velocity in a triply periodic domain. In Sec. III, we present the model for the unresolved contribution to the relative velocity of small inertial particles. In this section, the coupling of this model with the LES fields is assessed by comparing statistics obtained from the Direct Numerical Simulations of [37] and the standard LES approach. In Sec. IV, we discuss the model for the fluctuating response time for particles larger than the Kolmogorov scale. This model is compared to the experiments of Refs. [11,21] and to standard LES with the Stokes drag law as well as its nonlinear correction for larger particle Reynolds number.

II. LES METHODOLOGY FOR THE CARRIER PHASE

We consider the transport of the particles by a statistically stationary, homogenous and isotropic turbulent flow. The flow is simulated by the LES approach using the standard Smagorinsky model [2,38] for the estimation of the turbulent viscosity: $\nu_\Delta = \Delta_\star^2 |\overline{S}_{ij}|$, where $\overline{S}_{ij}$ is the filtered rate of strain tensor, and $\Delta_\star = C_s \Delta$ is the mixing length of the model with Δ the cutoff scale of the simulation and C_s the Smagorinsky constant. We use a pseudospectral approach to compute the flow of the carrier phase [39,40] and the forcing of the flow is ensured by keeping constant the kinetic energy of the smallest wave numbers [41]. The 2/3 dealiasing technique acts as an explicit filtering of the fluid velocity field, as a consequence the cutoff scale is $\Delta = 3H/2N$, with H the size of the computational domain and N the number of mesh points in this direction.

The Reynolds number based on the Taylor length scale is $Re_\lambda \approx 400$ and 3 mesh resolutions are used: 128^3, 96^3, and 64^3. The ratio between the smallest resolved scale (Δ) and the Kolmogorov length scale (η) corresponds approximately to 20, 30, 50. For the three resolutions, the Smagorinsky

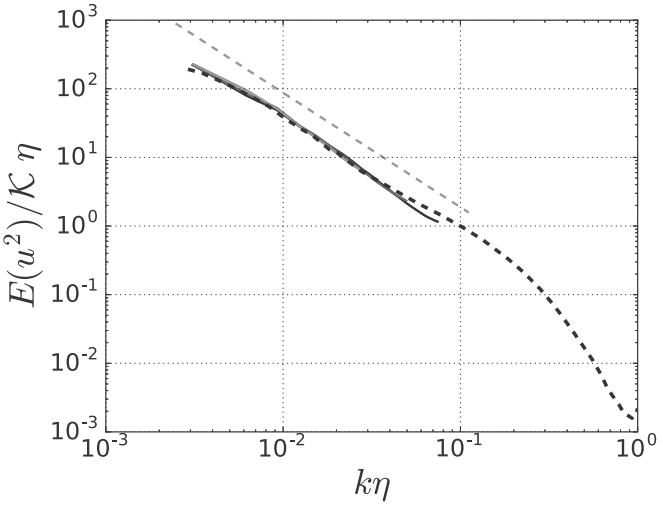

FIG. 1. Velocity spectra from the LES for 3 mesh resolutions 64^3 (light gray), 96^3 (gray), and 128^3 (black), and comparison with the DNS of Ref. [42] in dashed lines and the $k^{-5/3}$ power law in gray dashed lines.

constant is set to $C_s = 0.19$. Note that to resolve all scales at such Reynolds number, the Direct Numerical Simulations (DNS) of Refs. [37] and [42] require a mesh with 2048^3 points.

In Fig. 1 it is seen that the velocity spectra for the LES at the different resolutions are very close to the velocity spectra obtained from the DNS of Ref. [42] and present, as expected, the $-5/3$ slope, and for the three resolutions the cutoff scale lies in the inertial range. Details of the comparison of the flow from the various LES and the DNS are given in Table I. It is seen that for the three resolutions the LES is able to correctly estimate the turbulent length and time scale ratio obtained from the DNS.

From the filtered velocity field obtained from LES, the local instantaneous value of the dissipation rate $\varepsilon = 2\nu S_{ij} S_{ij}$ cannot be computed as it requires the knowledge of the local instantaneous velocity gradients. However, from the turbulent viscosity model, one can estimate the energy flux that cascades from scale Δ to smaller scales, and the total flux of energy at the scale of the mesh is $\varepsilon_\Delta = 2(\nu + \nu_\Delta)\overline{S}_{ij}\overline{S}_{ij}$. It should be noted that although the turbulent viscosity model ensures that the average flux is consistent: $\langle\varepsilon_\Delta\rangle = \langle\varepsilon\rangle$, ε_Δ exhibits much less intense fluctuations than ε (this will be illustrated in Fig. 5). For the Lagrangian tracking, the value of the fluid filtered fields is interpolated at the particles position with cubic splines [43]. Note that to avoid positivity issues, we interpolate the logarithm of ε_Δ.

TABLE I. Comparison of the numerical parameter and the flow characteristics of the LES at various resolutions 128^3, 96^3, and 64^3 and of the DNS of Ref. [37]. In the table, N is the number of mesh points in each direction, H is the size of numerical domain, $\tau_L = (2/3\mathcal{K})/\langle\varepsilon\rangle$ is the eddy turnover time, $L = (2/3\mathcal{K})^{3/2}/\langle\varepsilon\rangle$ is the scale of the large eddies, and $\mathcal{K}$ is the turbulent kinetic energy. $\mathrm{Re}_H = \sqrt{2/3\mathcal{K}}\,H/\nu$ is the Reynolds number based on the large scale of the flow, $\mathrm{Re}_\lambda = \sqrt{2/3\mathcal{K}}\,\lambda/\nu$ is the Reynolds number based on the Taylor length scale, $\eta = \nu^{3/4}\langle\varepsilon\rangle^{-1/4}$ and $\tau_\eta = \nu^{1/2}\langle\varepsilon\rangle^{-1/2}$ are the Kolmogorov length and time scales, respectively, and $\tau_\Delta = \Delta^2/\nu_\Delta$.

Type	N	Re_H	Re_λ	τ_L/τ_η	$\frac{\langle\varepsilon\rangle H}{\mathcal{K}^{3/2}}$	L/η	Δ/η	ν_Δ/ν	τ_Δ/τ_η
DNS	2048	21 800	420	111	1.09	1110	1.08	–	–
LES	128	20 800	408	105	1.02	1080	23.8	6.05	41.6
LES	96	20 600	398	103	1.07	1040	31.8	9.1	49.4
LES	64	20 100	389	100	1.09	1010	47.1	15.5	63.6

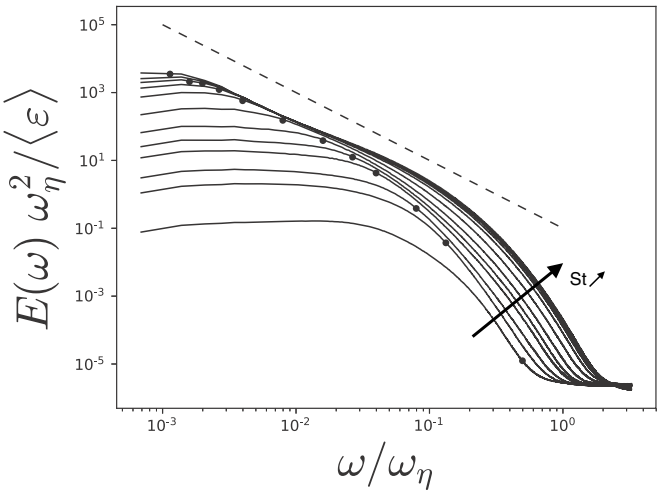

FIG. 2. Spectra of the particle relative velocity normalized using $\omega_\eta = 2\pi/\tau_\eta$ from the DNS of Ref. [37] at $\mathrm{Re}_\lambda = 420$ for various Stokes number (St = 0.16, 0.6, 1, 2, 3, 5, 10, 20, 30, 40, 50, 70). The dot indicates the nondimensional frequency ω_η/τ_p for each curve.

III. MODEL FOR A PARTICLE SMALLER THAN THE KOLMOGOROV SCALE

To emphasize the importance of the small-scale fluctuations in the motion of particles much smaller than the dissipative scale of the flow ($\Delta \gg \eta \gg d_p$), and to discuss further the estimation Eq. (2), we gather statistics from DNS of Toschi's group [37] at $\mathrm{Re}_\lambda = 420$. In this DNS only the Stokes drag force acts on the particles:

$$\mathbf{a}_p = \frac{\mathbf{u}_f - \mathbf{u}_p}{\tau_p}. \tag{4}$$

In Fig. 2, we present the Lagrangian spectra of the relative velocity $E(\omega)$ obtained from the DNS data of Ref. [37] for various Stokes numbers ranging from $\mathrm{St} = \tau_p/\tau_\eta = 0.16$ to 70. For vanishingly small Stokes number the relative velocity presents almost no fluctuation at all scales as expected, whereas increasing the Stokes number, an inertial range develops in which the spectra evolve as $E(\omega) \sim \langle\varepsilon\rangle\omega^{-2}$. In this figure, the main contribution of the fluctuations of the relative velocity is seen from frequency $\sim 1/\tau_p$ and higher. Such high-frequency fluctuations remain unresolved in LES.

The estimation Eq. (2), which takes place in the inertial interval of the turbulence spectrum, can be expressed as

$$\langle(\mathbf{u}_f - \mathbf{u}_p)^2\rangle \sim \langle\varepsilon\rangle\tau_p = \langle\varepsilon\rangle\tau_\eta \mathrm{St}. \tag{5}$$

This relation is compared with the data from the DNS of Ref. [37] in Fig. 3. It is observed that, at this Reynolds number, the prediction is correct over a narrow range of Stoke numbers.

To have an analytical estimation of $\langle(\mathbf{u}_f - \mathbf{u}_p)^2\rangle$ over a larger range of Stokes numbers, we consider first a particle with a vanishing response time ($\tau_p \ll \tau_\eta$). In that case the particles should behave as fluid tracers and one could estimate the variance of their acceleration as being of the order of $a_\eta^2 = \langle\varepsilon\rangle^{-3/2}\nu^{1/2}$. With Eq. (4) this leads to

$$\langle(\mathbf{u}_f - \mathbf{u}_p)^2\rangle = A\tau_p^2 a_\eta^2 = A\langle\varepsilon\rangle\tau_\eta \mathrm{St}^2. \tag{6}$$

The parameter $A = A(\mathrm{Re})$ accounts for the Reynolds number effect in the acceleration variance and according to Refs. [15,44] for $\mathrm{Re}_\lambda = 420$, $A \approx 3.9$. This evolution is also compared with the DNS data in Fig. 3 and is seen valid for $\tau_p \ll \tau_\eta$.

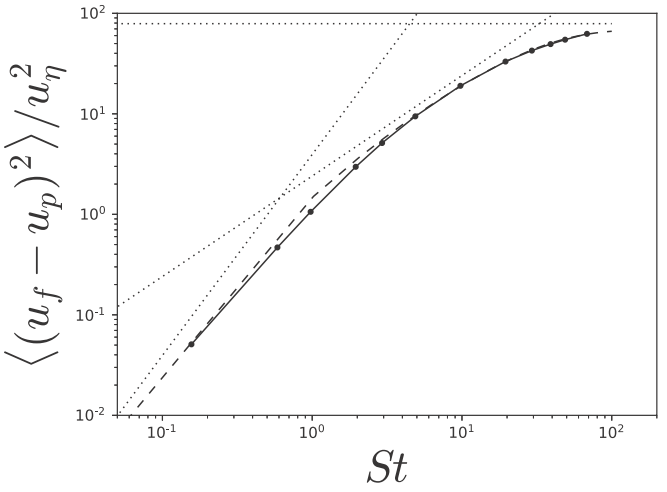

FIG. 3. Variance of the particle relative velocity normalized by $u_\eta^2 = \langle\varepsilon\rangle\tau_\eta$ as a function of the Stokes number from the DNS of Ref. [37] and comparison with the relations Eqs. (5), (6), and $2/3\,\mathcal{K}/u_\eta^2$ in dotted lines and with Eq. (9) in dashed lines.

By asymptotic matching of Eqs. (5) and (6), one can propose the following relation, valid for $\tau_p \ll \tau_L$:

$$\langle(\mathbf{u}_f - \mathbf{u}_p)^2\rangle \sim \langle\varepsilon\rangle\tau_\eta \frac{\mathrm{St}^2}{\mathrm{St}+1}. \tag{7}$$

Of course, this simple relation is not expected to reproduce exactly the DNS, as it does not account for preferential concentration effects, which have been shown in Ref. [45] to affect the statistics of the particle acceleration mainly for $\mathrm{St} = O(1)$. Nevertheless, in Fig. 3 this relation is seen to reproduce reasonably well the variance of the relative velocity.

On the other side, for particle inertia much larger than the integral time scale of the flow, $\tau_p \gg \tau_L$, the relative velocity variance approaches the variance of the fluid velocity. Then asymptotically, let us assume the following expression:

$$\langle(\mathbf{u}_f - \mathbf{u}_p)^2\rangle \approx \tfrac{2}{3}\mathcal{K}[1 - \exp(-\tau_p/\tau_L)], \tag{8}$$

where $\mathcal{K}$ is the mean turbulent kinetic energy of the fluid. Finally, noting that for $\tau_p/\tau_L \ll 1$, $1 - \exp(-\tau_p/\tau_L) \approx \tau_p/\tau_L = \mathrm{St}\ \tau_\eta/\tau_L$, and that $\mathcal{K} = \langle\varepsilon\rangle\tau_L$, the following relation is proposed for the variance of the particle relative velocity:

$$\langle(\mathbf{u}_f - \mathbf{u}_p)^2\rangle \approx \frac{2}{3}\langle\varepsilon\rangle\tau_L(1 - \exp(-A\,\tau_p/\tau_L))\frac{\mathrm{St}}{\mathrm{St}+2/3}. \tag{9}$$

From Fig. 3, this expression appears to be reasonably accurate over the whole range of Stokes number. Recalling that $\frac{\tau_L}{\tau_\eta} \sim \mathrm{Re}^{1/2}$, it is straightforward from Eq. (4) to express the particle acceleration variance, as a function of the Stokes and Reynolds numbers:

$$\left\langle \mathbf{a}_p^2 \right\rangle \approx \frac{\langle\varepsilon\rangle}{\tau_\eta} \underbrace{\frac{2}{3}\left(\frac{1 - \exp(-A(\mathrm{Re})\,\mathrm{StRe}^{-1/2})}{\mathrm{StRe}^{-1/2}(\mathrm{St}+2/3)}\right)}_{f^2(\mathrm{St},\mathrm{Re})}. \tag{10}$$

In line with the refined Kolmogorov hypothesis [46,47] and following Refs. [14] and [15], it is inferred that the main source of fluctuations in the particle acceleration is attributed to the large fluctuations of the local value of the dissipation rate. Therefore, from the previous relation Eq. (10)

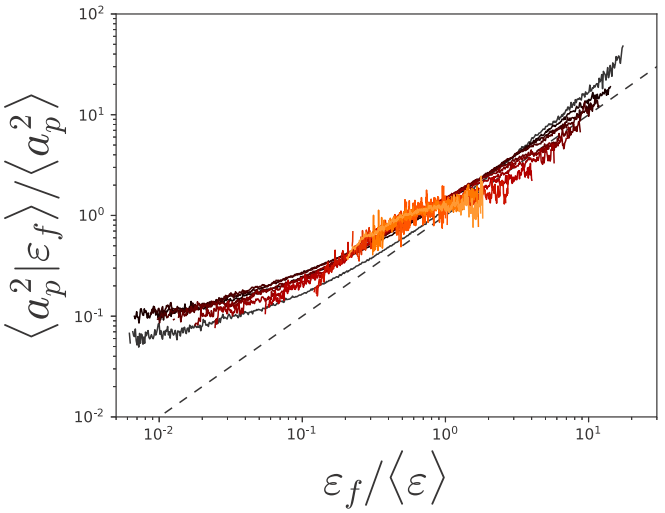

FIG. 4. Variance of the particle acceleration conditional to the temporally filtered local rate of dissipation, for various Stokes numbers from St = 0 to 70 from black to orange.

it is proposed to express the particle acceleration variance conditioned on the local dissipation rate "seen" by the particle ε_f:

$$\langle \mathbf{a}_p^2 | \varepsilon_f \rangle \sim \frac{\varepsilon_f}{\tau_\eta} f^2(\mathrm{St},\mathrm{Re}), \tag{11}$$

where ε_f is the value of ε along the particle trajectory filtered at the time scale of the particle τ_p: $\varepsilon_f = G_{\tau_p} * \varepsilon$, G_{τ_p} being the kernel of the filter with characteristic time τ_p. This behavior is confirmed in Fig. 4, where it is observed that the conditional acceleration variance presents a close to linear behavior with ε_f. Similarly to the numerical finding of Ref. [15] for fluid particles, the conditional acceleration variance deviate from the straight line prediction for small fluctuations of ε_f. But, more importantly, we observe that for all the Stokes number, the curves present the same behavior. Equation (11) is used further for the construction of the stochastic model for the particle acceleration at unresolved scales.

As discussed in the Introduction, Eq. (3) is proposed to express the instantaneous particle acceleration, as the sum of a filtered and stochastic contributions. Based on the time-scale separation between the evolution of the norm and the orientation observed experimentally [48] and proposed for fluid particles in Refs. [28,49], the unresolved contribution is expressed by the product of two stochastic processes, one for the amplitude of the particle residual acceleration $|a|_*$ and the other for its orientation vector $\mathbf{e}_*$:

$$\mathbf{a}_p = \underbrace{\widehat{\mathbf{a}}_p}_{\substack{\text{large scale}\\ \text{contribution}}} + \underbrace{|a|_* \mathbf{e}_*}_{\substack{\text{random}\\ \text{contribution}}} . \tag{12}$$

Consistently with Eqs. (10) and (11), the model for $|a|_*$ is given by

$$|a|_* = k_1 \varepsilon_*^{1/2} \tau_\eta^{-1/2} f(\mathrm{St},\mathrm{Re}_{\Delta_\star}). \tag{13}$$

To account for the Reynolds number at the unresolved scale of the flow, in contrast with Eq. (10), where f is defined, in the previous equation the argument of f is $\mathrm{Re}_{\Delta_\star} = (\tau_{\Delta_\star}/\tau_\eta)^2$, where $\tau_{\Delta_\star} = \Delta_\star^2/\nu_\Delta$ is the smallest resolved time scale. The value of $k_1 = 2$ is checked to give the best agreement with the DNS as seen later. In Eq. (13), ε_* denotes the local dissipation rate "seen" by a particle. To estimate its evolution along the particle trajectory, ε_* follows a stochastic process that depends on

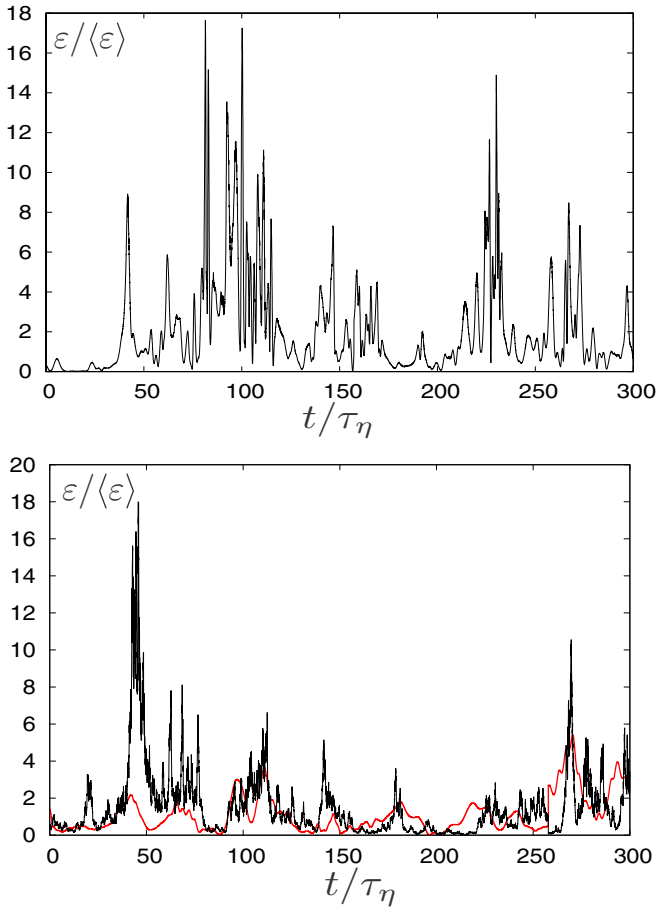

FIG. 5. (Top) A realization of the evolution of ϵ along a particle trajectory at $\mathrm{St} = 1$ and $\mathrm{Re}_\lambda = 420$, from the DNS of Ref. [37]. (Bottom) In red, a realization of the evolution of ϵ_Δ along a particle trajectory at $\mathrm{St} = 1$ and $\mathrm{Re}_\lambda = 420$, from the LES with a 64^3 mesh; in black, a realization of the stochastic process for ε_*.

the local value of ε_Δ computed from coarse LES mesh. Assuming a log-normal distribution for ε_*, one obtained the following stochastic process for $\varepsilon_*^{1/2}$ (see Appendix A):

$$\frac{d\varepsilon_*^{1/2}}{\varepsilon_*^{1/2}} = \frac{d\varepsilon_\Delta^{1/2}}{\varepsilon_\Delta^{1/2}} - \ln\left(\frac{\varepsilon_*^{1/2}}{\varepsilon_\Delta^{1/2}}\right)\frac{dt}{\tau_{\Delta_\star}} + \sqrt{\frac{1}{2}\frac{\sigma^2}{\tau_{\Delta_\star}}}dW, \tag{14}$$

with dW the increment of the Wiener process. The parameter σ in Eq. (14) is set to $\sigma^2 = \frac{1}{2}\ln\frac{\tau_{\Delta_\star}}{\tau_\eta+\tau_p}$. It is seen that that with increasing τ_p, the variance σ^2 decreases to mimic the filtering of the local value of the dissipation rate operated by the particle inertia, whereas for vanishing τ_p, we have $\sigma^2 = 1/4\ln\mathrm{Re}_\Delta$ which reproduces the DNS results of [50]. For illustration, in Fig. 5, we compared the dissipation rate "seen" by a particle along its path from the DNS of Ref. [37] and the energy flux ε_Δ from LES with a sample path from Eq. (14). It is seen that the stochastic process Eq. (14) presents large fluctuations in agreement with the behavior observed by DNS.

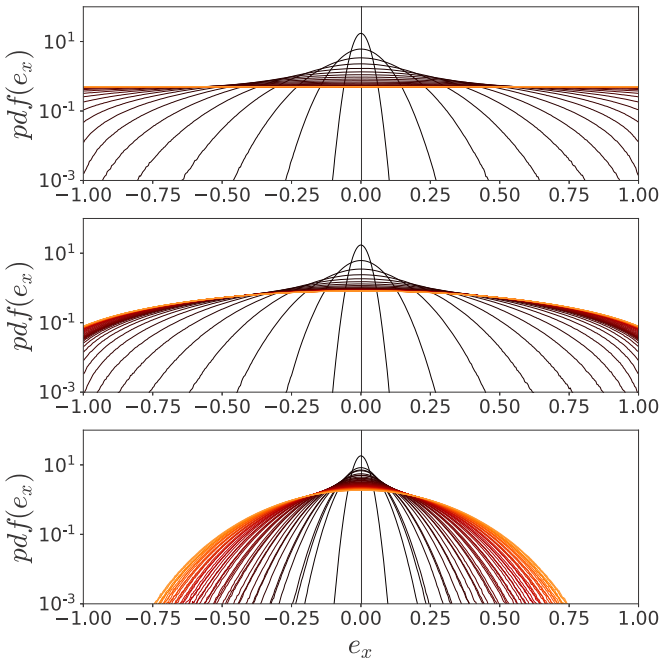

FIG. 6. Evolution of the PDF of the component $\mathbf{e}_x$ of the orientation vector as given by the stochastic model Eqs. (15) and (16), where the relaxation term is expressed $\overline{\mathbf{a}}_p/\Delta_\star = \mathbf{e}_{\rm eq}/\tau_R^2$ for three values of τ_R: $\tau_R = \infty$, 0.5 and 0.1, respectively, from top to bottom. In each case: $e_{\rm eq} = (0,0,+1)$, the initial orientation is $\mathbf{e}_x(t=0) = (0,0,+1)$, $\sigma_e^2 = 1$, $\tau_e = 1$. Each curve corresponds to a different instant from $t = 0$ to $t = 5\tau_e$, respectively, from black to orange, and separated by a time interval of $0.1\tau_e$.

In Eq. (12), the model for the orientation vector $\mathbf{e}_*$, is given by a random process on a unit sphere [29,51,52]:

$$d\boldsymbol{\alpha} = -\mathbf{e}_* \times \frac{\widehat{\mathbf{a}}_p}{\Delta_\star} dt - \boldsymbol{\alpha}\frac{dt}{\tau_e} + \sqrt{\frac{\sigma_e^2}{\tau_e}} d\mathbf{W}, \tag{15}$$

$$d\mathbf{e}_* = \gamma\, \mathbf{e}_* \times \boldsymbol{\alpha} dt + (\gamma - 1)\mathbf{e}_*. \tag{16}$$

In this process, the orientation $\mathbf{e}_*$ is modified by a random angular displacement $\boldsymbol{\alpha}dt$. In Eq. (16), the factor $\gamma = [1 + (\boldsymbol{\alpha}dt)^2 - (\mathbf{e}_* \cdot \boldsymbol{\alpha}dt)^2]^{-1/2}$ corresponds to a projection ensuring that the norm of the orientation vector remains unity (see Appendix B for details). The orientation increments are obtained from the angular velocity $\boldsymbol{\alpha}$ of a point on the surface of the sphere which evolves according to the Ornstein-Uhlenbeck process given in Eq. (15). This stochastic process is composed of relaxation, damping, and diffusion terms. The diffusion term, in which $d\mathbf{W}$ is a 3D Wiener process ($\langle dW_i \rangle = 0$ and $\langle dW_i dW_j \rangle = dt\delta_{ij}$), ensures the tendency to return toward a statistically isotropic orientation by allowing the vector $\mathbf{e}_*$ to take all possible orientation. The damping term is necessary to control the rate of return to isotropy at short time lag. In contrast to the return to isotropy, the relaxation term in Eq. (15) tends to align $\mathbf{e}_*$ with the orientation of the large-scale contribution of the particle acceleration $\widehat{\mathbf{a}}_p/|\widehat{\mathbf{a}}_p|$ with a relaxation rate dependent on its magnitude: $(|\widehat{\mathbf{a}}_p|/\Delta_\star)^{-1/2}$. The contribution of the different terms is illustrated in Fig. 6, which presents the evolution of the PDF of a component of the orientation vector. It is seen that without the relaxation term each orientation becomes equiprobable, while increasing the intensity of the relaxation term leads to a narrower stationary distribution. The parameters are $\tau_e = \frac{1}{2}(\tau_p + \tau_\eta)$ and $\sigma_e^2 = \tau_e^{-2}$. With this process, when

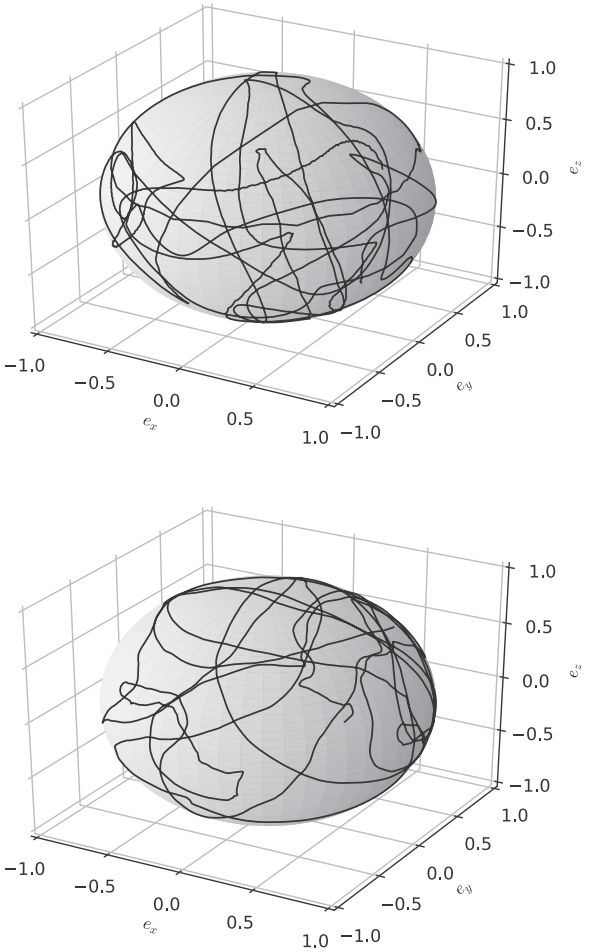

FIG. 7. (Top) Evolution of the orientation vector of the acceleration of a particle with $\mathrm{St} = 0.6$ and $\mathrm{Re}_\lambda = 420$, from the DNS of Ref. [37]. (Bottom) A realization of the random orientation $\mathbf{e}_*$ for $\mathrm{St} = 0.6$ and $\mathrm{Re}_\lambda = 420$ and a 64^3 LES mesh. For both panels, the observation time span over $100\tau_\eta$.

$\tau_e \ll (|\widehat{\mathbf{a}}_p|/\Delta_\star)^{-1/2}$ the orientation becomes practically independent of the large-scale orientation, consistently with the assumption of local isotropy in the small scales of large Reynolds number flow; otherwise, for $\tau_e \gg (|\widehat{\mathbf{a}}_p|/\Delta_\star)^{-1/2}$, the orientation is impressed by the large resolved scales.

The combination of these terms is necessary to have the autocorrelation of the acceleration orientation consistent with the experiments and the DNS, as discussed later (see Fig. 7). For vanishingly small Stokes number the correlation time for the acceleration components is commensurate with τ_η as in the experiments of Ref. [48], while increasing St leads to an increase in the correlation time. Because the stochastic orientation $\mathbf{e}_*$ is correlated with the "resolved" acceleration, the two stochastic processes for the modulus and for the orientation are not independent. Finally, note that this model share some similarities with the Debye model [53,54].

Concerning the resolved contribution in Eq. (12), the particle acceleration is computed from the spatially filtered fluid velocity field $\overline{\mathbf{u}}_f$ obtained from the coarse LES mesh. Moreover, an explicit temporal filtering is applied to obtain the large scale contribution:

$$\widehat{\mathbf{a}}_p = G_{\tau_{\Delta_\star}} * \left(\frac{\overline{\mathbf{u}}_f - \mathbf{u}_p}{\tau_p} \right), \tag{17}$$

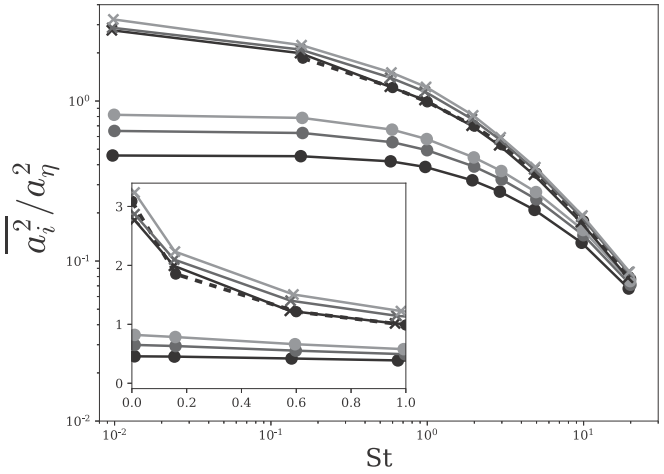

FIG. 8. Variance of the particle acceleration normalized by the Kolmogorov acceleration ($a_\eta^2 = \langle\varepsilon\rangle^{3/2}\nu^{-1/2}$) in logarithm scale. Crosses, LES with the proposed model; circles, LES without model; for the three meshes, 64^3 (black), 96^3 (dark gray), and 128^3 (light gray). Comparison with the DNS of Ref. [37] in dashed line. Inset zoom for small Stokes number in linear scale.

where $G_{\tau_{\Delta_\star}}$ is a temporal filtering kernel with characteristic time $\tau_{\Delta_\star}$. Of course, if only the resolved contribution is accounted for in the particle dynamics (i.e., without model for the unresolved contribution) this explicit temporal filtering is useless since no fluctuations with frequency larger than the cutoff frequency of $\overline{\mathbf{u}}_f$, which is of order $\tau_{\Delta_\star}^{-1}$, can develop. However, with the stochastic forcing in the particle acceleration, it becomes necessary to apply an explicit temporal filter, to prevent the resolved term to respond with high frequency oscillations. The implementation of this temporal filter is straightforward. It is sufficient to replace the relaxation time scale τ_p in the resolved contribution by $\tau_{\Delta_\star}$ whenever $\tau_p < \tau_{\Delta_\star}$:

$$\overline{\frac{d\mathbf{u}_p}{dt}} = \frac{\overline{\mathbf{u}}_f - \mathbf{u}_p}{\max(\tau_{\Delta_\star}, \tau_p)}. \tag{18}$$

From the standard LES (for which no explicit temporal filtering is applied) it is observed for the three resolutions and for $\tau_p < \tau_{\Delta_\star}$ that the particle acceleration variance becomes independent of the Stokes number (see Fig. 8).

A. Assessment of the model

To validate this approach, we present comparisons of statistics of the particle dynamics obtained from the LES with the proposed model Eqs. (12)–(18), the DNS of Ref. [37] and the standard LES approach without a model for accounting of the subgrid scale fluctuations.

First, we consider in Fig. 8 the particle acceleration variance. It is observed that the standard LES approach fails to reproduce the acceleration variance obtained with DNS. As expected, the coarser the LES mesh, the larger the underestimate of the variance. With the coarsest LES mesh, the variance of particles with small Stokes number is approximately 10 times smaller than for the DNS. Furthermore, as discussed above the acceleration variance predicted by the LES saturate when $\tau_p < \tau_{\Delta_\star}$. This is in contrast with the LES supplemented with the proposed stochastic model, for which the agreement with the DNS is fairly good over the whole range of Stokes number considered. Moreover, it is seen that this accurate prediction holds for the three meshes resolutions tested here. Therefore, this indicates that, with the model for the residual acceleration, the LES becomes nearly independent of the mesh resolution which implies that the proposed model accurately reproduce the

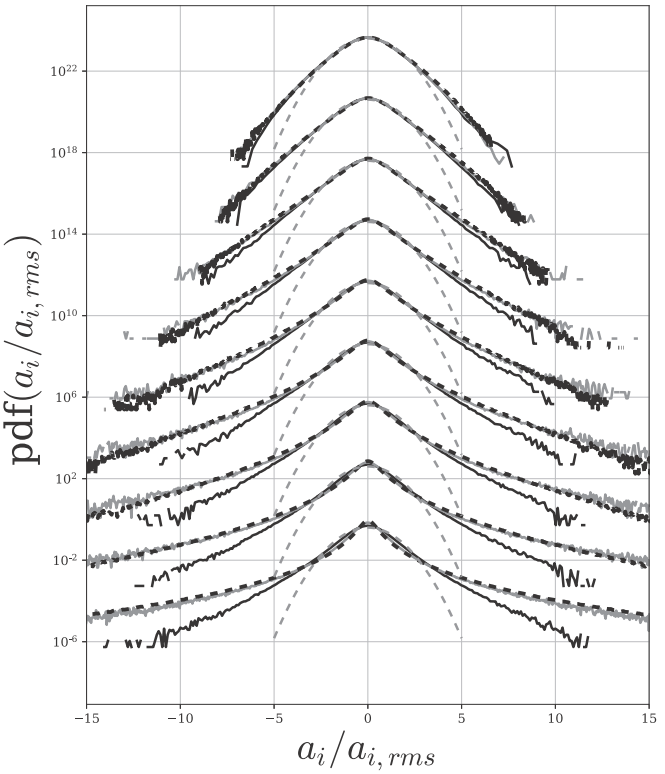

FIG. 9. PDF of the particle acceleration normalized by its variance for St = 0.016, 0.16, 0.6, 1, 2, 3, 5, 10, 20 (respectively, shifted upward by one decade from each other for clarity). Gray, LES at 64^3 with the proposed model; black, LES at 64^3 without models; black dashed line, DNS of Ref. [37]; gray dashed line, the Gaussian distribution.

effect of the unresolved small scales of the flow. Note that very similar trends are observed for the variance of the acceleration modulus but are not shown for brevity.

In Fig. 9, we present the PDF of the particle acceleration for the various Stokes numbers. As expected [45], for small Stokes numbers, the PDF obtained from the DNS exhibits non-Gaussian behavior, with very stretched tails, whereas the distribution becomes narrower as the Stokes number increases. With the proposed model the LES simulation is able to predict this behavior remarkably well, while without the model the LES cannot reproduce the largest fluctuations of the acceleration at small and moderate Stokes number. The good agreement between the LES with the model and the DNS is confirmed in Fig. 10, where the flatness of the particle acceleration is compared. Consistently with the observation of the PDF, it is seen that the flatness for small Stokes number is correctly estimated by the LES with the model, for all the three mesh resolutions and is largely underestimated by the standard LES, even with the fine mesh.

These findings strongly support the model Eqs. (12)–(18) and the choice of parameters.

Figure 11 shows the autocorrelation of the particles acceleration along their trajectory. It is observed that, for both small and moderate Stokes numbers, the LES without model provides a too slow decorrelation of the acceleration compared with the DNS. With the proposed model, the LES presents a shorter correlation time, in agreement with the DNS. This is due to the high-frequency forcing provided by the stochastic model. Also important to obtain realistic autocorrelation is the specific orientation model provided in Eqs. (15) and (16) and in particular the correlation between

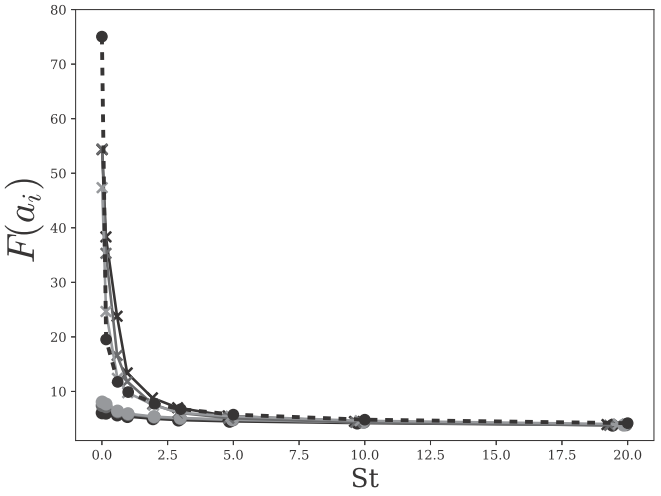

FIG. 10. Flatness of the particle acceleration. Crosses, LES with the proposed model; circles, LES without models; for the three meshes, 64^3 (black), 96^3 (dark gray), and 128^3 (light gray). Comparison with the DNS of Ref. [37] in dashed line.

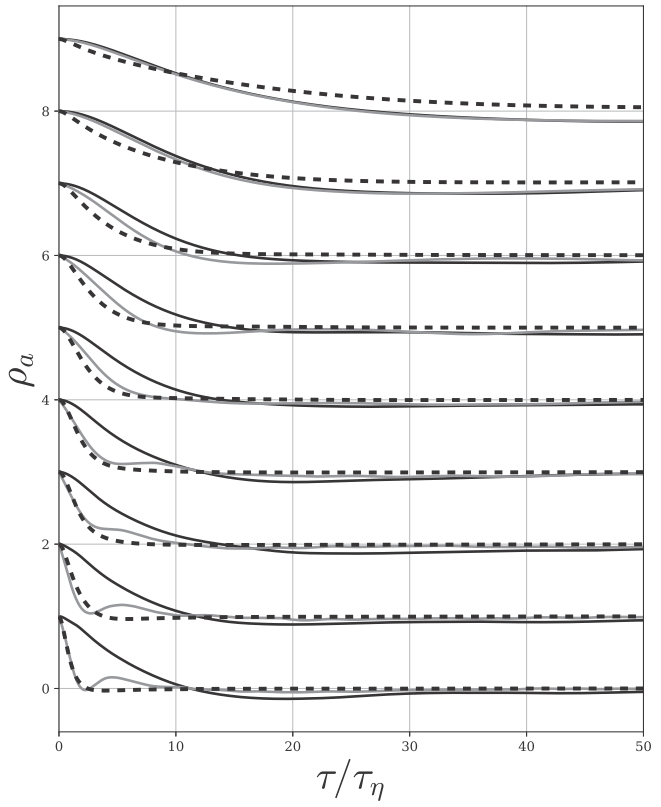

FIG. 11. Auto-correlation of the particle acceleration for $\mathrm{St} = 0.016, 0.16, 0.6, 1, 2, 3, 5, 10, 20$ (respectively, shifted upward by one unit each other). Gray, LES at 64^3 with the proposed model; black, LES at 64^3 without the model; black dashed line, DNS of Ref. [37].

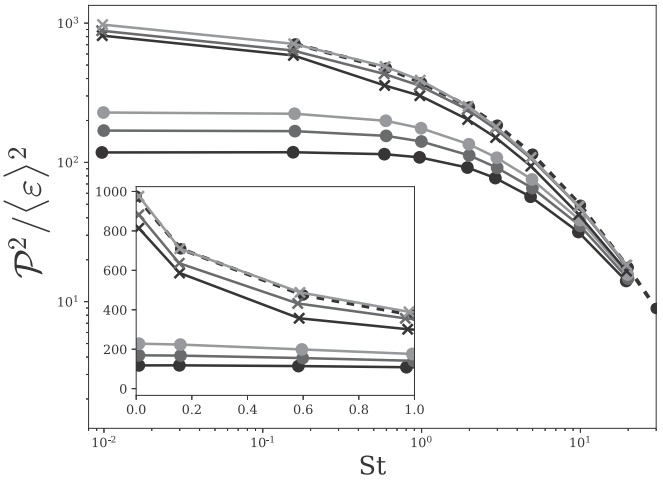

FIG. 12. Variance of the power exchange with the fluid per unit mass of a particle normalized by the mean dissipation rate in logarithm scale. Crosses, LES with the proposed model; circles, LES without the model; for the three meshes, 64^3 (black), 96^3 (dark gray), and 128^3 (light gray). Comparison with the DNS of Ref. [37] in dashed line. Inset zoom for small Stokes number in linear scale.

the orientation model and the resolved orientation as well as the explicit temporal filtering of the resolved part of the particle acceleration.

We also consider the statistics of the rate of change of the kinetic energy of a particle $d(\mathbf{u}_p^2/2)/dt = \mathbf{a}_p \cdot \mathbf{u}_p = \mathcal{P}$. Since in the absence of other forces, this quantity is the power (per unit mass of a particle) received by a particle from the fluid, it characterizes the interaction of the particles with the fluid phase. In Fig. 12 we present the variance of the power fluctuations normalized by the mean dissipation rate $\langle\mathcal{P}^2\rangle/\langle\varepsilon\rangle^2$. Consistently with the observation of Ref. [55] for fluid tracers, we remark that according to the DNS, the characteristic power fluctuations are much larger than $\langle\varepsilon\rangle$. It is also observed in this figure that LES without the model under-predicts by almost one order of magnitude the variance of the power fluctuations for $\mathrm{St} < 5$, whereas with the LES supplemented by the model for small scale agitation, the prediction follows remarkably well the DNS and does not present effects of the mesh resolution. Due to the stationarity of the flow, the average power is zero, but the skewness of the distribution is negative, as pointed out by Ref. [55]. This is seen in the PDF of $\mathcal{P}$, in Fig. 13, which also present very stretched tails, especially for small Stokes numbers. Again such tails, as well as their dissymmetry can be fairly well reproduced by the LES coupled with the small scales model, while LES without the model gives less developed tails. As apparent from its definition, $\mathcal{P}$ depends on the correlation between the resolved and small-scale contributions as well as the orientation and magnitude of the modeled part. Therefore, the good agreement observed validate the proposed modeling strategy.

IV. STOCHASTIC RESPONSE TIME FOR A PARTICLE LARGER THAN THE KOLMOGOROV SCALE

In this section we consider a particle that is larger than the Kolmogorov length scale of the flow but that remain much smaller than the grid scale: $\Delta \gg d_p \gg \eta$. In this situation the turbulent eddies, of sizes from d_p to η, drag collectively such a particle due to the fluid-particle relative motion. It is then natural to assume that statistically this drag is characterized by an effective viscosity of the turbulent flow at the scale of the particle d_p. On the other hand, instantaneously, the strong fluctuations of the flow structures at scales of order d_p may cause an additional source of agitation for the particle, despite its significant inertia. To account for turbulent fluctuations in the drag of a "large-subgrid"

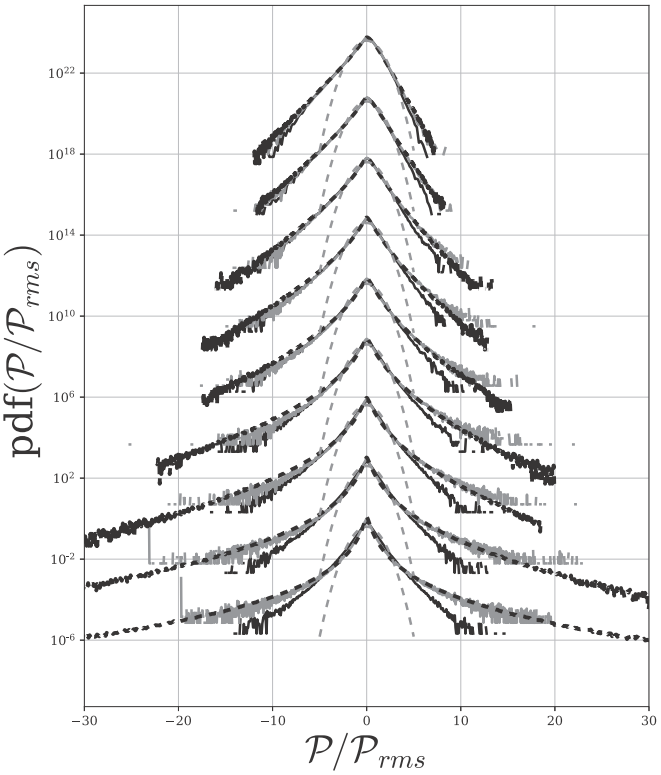

FIG. 13. PDF of the power exchange with the fluid normalized by its variance for St = 0.016, 0.16, 0.6, 1, 2, 3, 5, 10, 20 (respectively, shifted upward by one decade from each other for clarity). Gray, LES at 64^3 with the proposed model; black, LES at 64^3 without the model; black dashed line, DNS of Ref. [37]; gray dashed line, Gaussian distribution.

particle, we propose to introduce an effective response time $\tau_{p,t}$:

$$\tau_{p,t} = \frac{\rho_p}{\rho_f} \frac{d_p^2}{18(\nu + \nu_{p,t})}, \tag{19}$$

where $\nu_{p,t}$ is defined as the turbulent viscosity at the scale of the particle. Using the Prandtl's mixing length hypothesis and Kolmogorov scaling, we have $\nu_{p,t} \sim u' d_p \sim \langle \varepsilon \rangle^{1/3} d_p^{4/3}$ Furthermore, following the refined Kolmogorov hypothesis [46,47], we introduce a turbulent viscosity defined locally, along the particle path, based on the energy flux from scale d_p to smaller scales, ε_d:

$$\nu_{p,t} \sim \varepsilon_d^{1/3} d_p^{4/3}. \tag{20}$$

With this expression one gets, for the turbulent response time,

$$\frac{1}{\tau_{p,t}} = \frac{1}{\tau_p} + 18 \frac{\rho_f}{\rho_p} \frac{\varepsilon_d^{1/3}}{d_p^{2/3}}. \tag{21}$$

In the framework of the decomposition introduced previously, Eqs. (12) and (13), but with using now the turbulent response time Eq. (21), the resolved and subgrid contributions for the acceleration become

$$\mathbf{a}_p = \frac{\overline{(\mathbf{u}_f - \mathbf{u}_p)}}{\tau_{p,t}} + \left(\frac{\varepsilon_d}{\tau_{p,t}} \right)^{1/2} \mathbf{e}_*. \tag{22}$$

We assumed in Eq. (22) and in the following that $\tau_L \gg \tau_{p,t} \gg \tau_\eta$, to use the simplified estimation of the relative velocity given by Eq. (5). With Eq. (21) this relation reads

$$\mathbf{a}_p = \overline{\frac{(\mathbf{u}_f - \mathbf{u}_p)}{\tau_p}} + 18\overline{\frac{\rho_f}{\rho_p}\frac{\varepsilon_d^{1/3}}{d_p^{2/3}}(\mathbf{u}_f - \mathbf{u}_p)} + \left(\frac{\varepsilon_d}{\tau_p} + 18\frac{\rho_f}{\rho_p}\frac{\varepsilon_d^{4/3}}{d_p^{2/3}}\right)^{1/2}\mathbf{e}_*. \tag{23}$$

To further simplify this expression, note that for $d_p \gg \eta$, $\nu_{p,t} \gg \nu$ and therefore the subgrid scale contribution is dominated by the fluctuating response time ($\frac{\rho_f}{\rho_p}\frac{\varepsilon_d^{4/3}}{d_p^{2/3}} \gg \frac{\varepsilon_d}{\tau_p}$). Second, as specified above, we consider that $\Delta \gg d_p$, which as in the previous section, implies that the unresolved scale dominates in the estimation of the relative velocity: $(\varepsilon_d d_p)^{1/3} \gg |\overline{\mathbf{u}_f - \mathbf{u}_p}|$. With these assumptions, Eq. (23) becomes

$$\mathbf{a}_p = \overline{\frac{(\mathbf{u}_f - \mathbf{u}_p)}{\tau_p}} + \left(18\frac{\rho_f}{\rho_p}\right)^{1/2}\frac{\varepsilon_d^{2/3}}{d_p^{1/3}}\mathbf{e}_*. \tag{24}$$

For very large Reynolds number, one can neglect the filtered part and it is seen from Eq. (24) that the particle acceleration variance for $d_p \gg \eta$ scales as

$$\langle a_p^2 \rangle \sim \frac{\rho_f}{\rho_p}\frac{\langle \varepsilon^{4/3} \rangle}{d_p^{2/3}}. \tag{25}$$

This is consistent with the $d^{-2/3}$ scaling proposed by Refs. [5,11,21] for nearly buoyant particles and for particle density ratio up to 50. Note that the intermittency correction to this scaling suggested in Ref. [21], which leads to a possible $d_p^{-0.8}$ dependence, is discussed later. Furthermore, note that when $d_p \gg \Delta$, the second term on the right-hand side of Eq. (23) should dominate and the variance of the acceleration scale like $\langle a_p^2 \rangle \sim (\rho_f/\rho_p)^2 \langle (\mathbf{u}_f - \mathbf{u}_p)^2 \rangle \langle \varepsilon \rangle^{2/3} d_p^{-4/3}$, which is in agreement with the $\sim d_p^{-4/3}$ dependence observed in Refs. [56,57] for large particles dominantly swept by the large scales of the flow. Of course, this limit is beyond the validity of the "large pointwise" particle approach considered in this paper.

Similarly to the previous section, the model Eq. (24) requires the knowledge of the instantaneous energy flux seen by the particle along its trajectory. Assuming a log-normal statistics for ε_d one obtains a surrogate process with the following stochastic equation for $\varepsilon_d^{2/3}$ (see Appendix A):

$$\frac{d\varepsilon_d^{2/3}}{\varepsilon_d^{2/3}} = \frac{d\varepsilon_\Delta^{2/3}}{\varepsilon_\Delta^{2/3}} - \left(\ln\frac{\varepsilon_d^{2/3}}{\varepsilon_\Delta^{2/3}} + \frac{2}{9}\sigma^2\right)\frac{dt}{\tau_{\Delta_\star}} + \sqrt{\frac{8}{9}\frac{\sigma^2}{\tau_{\Delta_\star}}}dW, \tag{26}$$

where as previously $\tau_{\Delta_\star} = \Delta_\star^2/\nu_\Delta$ and $\sigma^2 = \frac{1}{2}\ln \tau_{\Delta_\star}/\langle \tau_{p,t} \rangle$, which should yield a reduction of the occurrence of large fluctuations of the particle acceleration with increasing the particle size, as observed by Ref. [21]. It may be noted that because of the dependence of σ^2 on d_p, one should also consider an intermittency correction to the scaling of $\langle a_p^2 \rangle$ with the particle diameter. From expressions for moments of lognormal distribution Eq. (A1) we have $\langle \varepsilon^{4/3} \rangle = \langle \varepsilon \rangle^{4/3} \exp(2/9\sigma^2)$, and with the proposed expression of σ^2 we find, for $\nu_{p,t} \gg \nu$, $\langle a_p^2 \rangle \sim d_p^{-2/3-2/27} = d_p^{0.74}$ against the $d_p^{-0.8}$ law proposed in Ref. [21].

The stochastic model for the orientation of the subgrid contribution $\mathbf{e}_*$ in Eq. (24) is $d_p^{**} - 0.744$ given by Eqs. (15) and (16) as in the case of the small particles with a similar definition of the parameters $\tau_e = \frac{1}{2}(\langle \tau_{p,t} \rangle + \tau_\eta)$ and $\sigma_e^2 = \tau_e^{-2}$. And, finally, the resolved part in Eq. (24) remains evaluated by Eq. (18), as in the previous section.

A. Assessment of the model

The evaluation of the model Eqs. (24)–(26) proposed for the particles larger than the Kolmogorov scale is given here by presenting statistics of the particle acceleration for particles with a diameter

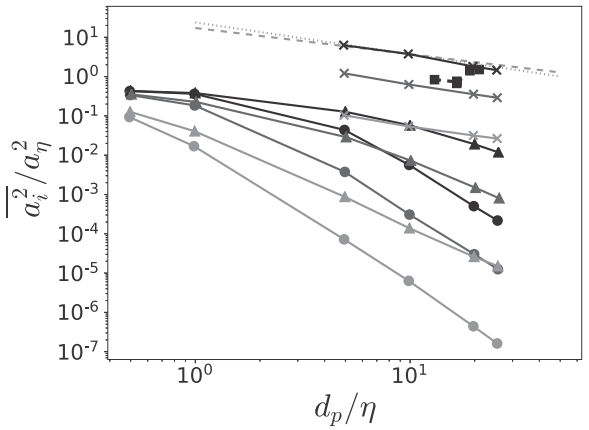

FIG. 14. Variance of the large particle ($\Delta > d_p > \eta$) acceleration normalized by the Kolmogorov acceleration ($a_\eta^2 = \langle\varepsilon\rangle^{3/2}\nu^{-1/2}$) in logarithm scale. Crosses, LES with the proposed model; circles, LES without the model with Stokes drag; triangles, LES without the model and with the drag correction of Schiller and Nauman. For three density ratios: $\rho_p/\rho_f = 50$ (black), 100 (dark gray), and 1000 (light gray). For all cases the mesh size is 64^3. Comparison with the experiments of Ref. [11] with particle density ratio around 50 in black squares and the power laws $\langle a_p^2\rangle d_p^{-2/3}$ in gray dashed line and $\langle a_p^2\rangle d_p^{-0.8}$ in gray dotted line.

of 5, 10, 20, and 26 η and for three density ratio $\rho_p/\rho_f = 50$, 100, and 1000. As pointed out in Refs. [56,57], the point-particle approximation with the usual drag law is clearly not valid for these sizes of particle. The results from the LES with the model are compared with experimental results from Refs. [8,11,21] and from standard LES approach, i.e., from LES without the model for unresolved fluctuations. Note that we expect the effect of gravity to be negligible in the experimental results of Refs. [8,11]. In the standard approach, two expressions for the particle response time are considered. The first one is the standard Stokes relaxation time $\tau_p = \rho_p/\rho_f d_p^2/18\nu$ valid for the small Reynolds number based on the particle diameter, $\mathrm{Re}_p < 1$, whereas in the second version the relaxation time accounts for the finite particle Reynolds number correction proposed from the experimental work of Schiller and Nauman [58] $\tau_p = \rho_p/\rho_f d_p^2/18\nu\,(1 + 0.15\ \mathrm{Re}_p^{0.687})^{-1}$ for $\mathrm{Re}_p = d_p|\mathbf{u}_p - \mathbf{u}|/\nu < 800$. Several papers, Refs. [23,59] for example, used this correction to account for the large size of the particles in turbulent flows.

The simulations presented here use a mesh size of 64^3. As seen in Table I, even the largest particle diameter considered here remains smaller than the grid spacing. Note that we consider only relatively heavy particles $\rho_p/\rho_f > 50$, because the added mass effects are not accounted for in this paper.

In Fig. 14, we present the acceleration variance as a function of the particle diameter for the various density ratio. It is seen that the two versions of the LES without models predict a strong reduction of the acceleration variance with increasing d_p/η. It is also seen that, as expected, in the case of the linear drag, the decrease is much more pronounced than in the case of the drag proposed by Schiller and Nauman. In contrast, from LES with the model Eqs. (24)–(26), the decrease of the acceleration variance with d_p/η is much less and presents a behavior similar to $d_p^{-2/3}$. For the short range of d_p/η considered here, the difference between $d_p^{-2/3}$ and $d_p^{-0.8}$ is not substantial but as expected for very large particle diameters the evolution appears closer to $d_p^{-0.8}$. In comparison with the standard approach, it is clearly seen that introduction of Eqs. (24)–(26) allowed us to match correctly the results of experiments in Ref. [8].

The PDF of the particle acceleration normalized by their standard deviation for $\rho_p/\rho_f = 50$ are given in Fig. 15. It is seen that the LES without model predicts a Gaussian distribution for the acceleration when the Stokes drag is used. This dramatically departs from the experimental findings, for which the tails of the PDF remain quite large even for large value of d_p/η. With the nonlinear drag

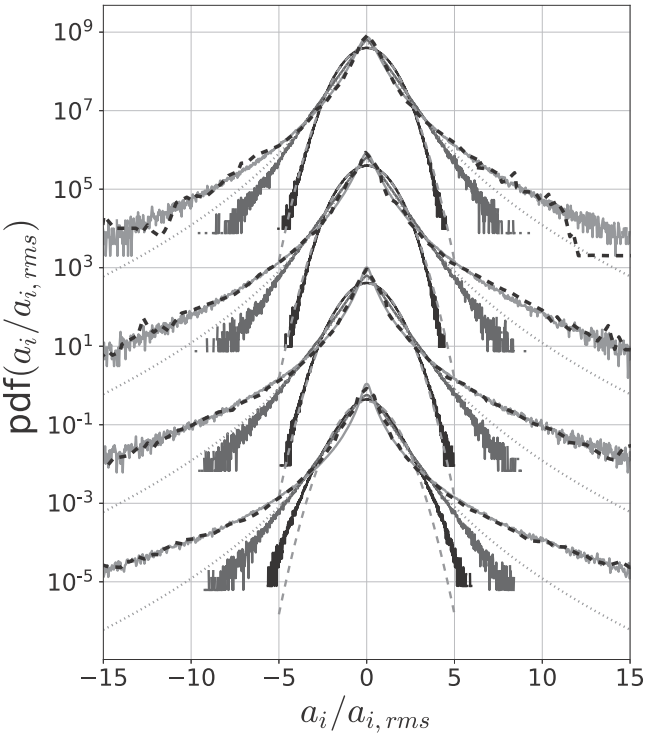

FIG. 15. PDF of the large particle ($\Delta > d_p > \eta$) acceleration normalized by its variance for $d_p/\eta = 5$,10, 20, and 26 (respectively, shifted upward by one decade from each other for clarity). Light gray, LES with the proposed model; black, LES without the model with Stokes drag; dark gray, LES without the model and with the drag correction of Schiller and Nauman. In each case, the density ratio is $\rho_p/\rho_f = 50$ and the mesh size 64^3. Comparison with the Gaussian distribution gray dashed line, with the experimental data of Ref. [21] (with $d_p/\eta = 1.6$, 8.2, 13.4, and 23.6) in black dashed line and with the fit from Ref. [11] in dotted line.

correction [58], the LES without model predicts a larger distribution, which surprisingly appears to be independent of the particle diameter. Nevertheless, the large fluctuations remain under-predicted compared to the experiments from both Refs. [11] and [21]. In contrast, the LES supplemented with the proposed stochastic model gives PDF tails in excellent agreement with the experiments of Ref. [21]. We would like to stress that although the experiments presented in Ref. [21] have been performed for nearly neutrally buoyant particles, it is believed that the dependence of the PDF tails on the particle diameters remains similar for not too dense particles. Note that in their experiments for particles with density ratio between 1 and 100, Refs. [8,11,20] observed that the shape of the PDF is left approximately invariant with a change of the particle diameter, at least for not too large fluctuations. However, it is to note that the PDF in Refs. [8,11,20] are observed to be less stretched compared to the PDF presented in Refs. [21,60] for similar size and density ratios and Reynolds numbers, pointing to some discrepancies between those experiments.

These favorable comparisons between LES with the model and the experiments support the proposed approach, although further comparisons with experiments and fully resolved numerical simulations appear necessary to establish the validity of the proposed model.

V. FINAL COMMENTS

In LES of turbulent flow laden with heavy particles, it is common practice to assume that the particle motion results from its response to the energy-containing large-scale eddies. However, recent

experiments, analytical estimations, and DNS showed that, in high Reynolds number flows, the large increments of velocity at small scales play an important role in the dynamics of particles even when their inertia is substantial. In this paper, we propose a new approach that accounts for the effects of the turbulent fluctuations at unresolved spatial scales ($<\Delta$) for both small ($\Delta \gg \eta \gg d_p$) and large ($\Delta \gg d_p \gg \eta$) particles. To this end, the instantaneous acceleration of the particle is decomposed into a large-scale contribution given by the resolved fluid velocity field and in a random contribution. The random part is obtained by the product of two stochastic processes. One is for the modulus and represents the particle acceleration conditionally averaged on the dissipation rate seen by a particle along its path. This latter quantity is assumed to follow a log-normal stochastic process. The expression of the acceleration modulus is derived from physical assumptions on the basis of the available DNS data. The second stochastic process is for the orientation of the particle acceleration and is given by a random walk on the unit sphere, ensuring the appropriate rate of return to the local isotropy.

We propose two models, valid for locally homogenous and isotropic high Reynolds number flows, to specifically estimate the subgrid scale contribution of the fluid-particle relative velocity and to reproduce the influence of the turbulent fluctuations at the scale of the particle. For particles larger than the Kolmogorov scale of the flow, we introduced a fluctuating particle response time base on an effective viscosity at the scale of the particle. The advantage of these models are demonstrated by comparisons with statistics obtained from the DNS of Ref. [37] in the case of the small particles ($\Delta \gg \eta \gg d_p$) and from the experiments of Refs. [11,21] for the large particles ($\Delta \gg d_p \gg \eta$). The evolution of the particle acceleration variance with the Stokes number or the particle diameter, the autocorrelation as well as its strongly non-Gaussian PDFs are in very good agreement with the DNS and the experiments in contrast with the standard tracking of the particles by LES. Finally, we stressed that the implementation of the proposed subgrid scale models is straightforward to implement.

Several extensions of this work can be considered. The stochastic process used to estimate the dissipation rate along the particle trajectory is independent from one particle to another and so the preferential concentration of the particles at subgrid scales cannot be reproduced by the modeling presented in this paper. The feedback of the particles on the carrier phase also is not accounted for here because we only considered vanishingly small volume fraction of particles. However, large particles generate vorticity in their wake which scales roughly as the particle Reynolds number [61–64], and the two-way coupling with surrounding turbulence may be of crucial importance. With the proposed models the momentum and energy transfer from the fluid to the particles is seen to be estimated fairly accurately, and thus it may also be useful to account for two-way coupling effects. To extend the range of validity of the approach to particles with smaller density ratio, it would be necessary to propose a modeling for the added mass and inertia terms which appears in the particle equation of motion. Finally, we note that the rotation of the particles has not been considered in this work, nevertheless it was shown recently [65] that the rotation could be important for the motion of large particles in a turbulent flow.

ACKNOWLEDGMENTS

We thank A. Lanottte, E. Calzavarini, F. Toschi, J. Bec, L. Biferale and M. Cencini for making the DNS dataset "Heavy particles in turbulent flows" (2011) publicly available from the International CFD Database [66]. M.G. and R.Z. gratefully thanks the support from the Center for Turbulence Research, Stanford University, and in particular the hospitality of Parviz Moin during the Summer Program 2014. M.G. also acknowledges the support from ANR Project-13-BS09-0009 LTIF.

APPENDIX A: LOG-NORMAL STOCHASTIC EQUATION FOR ε_*^n

Following the derivation of Ref. [27], we assume that the ratio $\varepsilon_*/\varepsilon_\Delta$ is log-normal where $\varepsilon_\Delta(t)$ evolves in time (with average value ε_0). Therefore, $\chi = \ln \varepsilon_*/\varepsilon_\Delta = \ln (\varepsilon_*/\varepsilon_0\, \varepsilon_0/\varepsilon_\Delta)$ follows

a Gaussian process: $d\chi = \Pi dt + \Sigma dW$ with dW the increment of a Wiener process ($\langle dW \rangle = 0$; $\langle dW^2 \rangle = dt$).

We introduce $f = (\varepsilon_*/\varepsilon_0)^n = (\varepsilon_\Delta/\varepsilon_0)^n e^{n\chi}$ and so $\frac{\partial f}{\partial \chi} = n(\varepsilon_\Delta/\varepsilon_0)^n e^{n\chi} = nf$, $\frac{\partial^2 f}{\partial \chi^2} = n^2(\varepsilon_\Delta/\varepsilon_0)^n e^{n\chi} = n^2 f$, and $\frac{\partial f}{\partial t} = nf \frac{d}{dt} \ln \varepsilon_\Delta/\varepsilon_0$.

Applying the Ito transform, the stochastic equation for f reads

$$\frac{df}{f} = \left(n \frac{d}{dt} \ln \frac{\varepsilon_\Delta}{\varepsilon_0} + n\Pi + \frac{n^2\Sigma^2}{2} \right) dt + n\Sigma dW.$$

Taking an Ornstein-Uhlenbeck process for χ of the form: $\Pi = -\frac{\chi - \mu}{\tau}$, $\Sigma = \sqrt{\frac{2\sigma^2}{\tau}}$, gives

$$\frac{df}{f} = \left(n\tau \frac{d}{dt} \ln \frac{\varepsilon_\Delta}{\varepsilon_0} - \ln \left[\left(\frac{\varepsilon_0}{\varepsilon_\Delta} \right)^n f \right] + n\mu + n^2\sigma^2 \right) \frac{dt}{\tau} + \sqrt{\frac{2n^2\sigma^2}{\tau}} dW.$$

The moments of f in the stationary state ($t \gg \tau$ and ε_Δ constant) are

$$\langle f^k \rangle = \exp\left(kn\mu + \frac{k^2 n^2 \sigma^2}{2} \right). \tag{A1}$$

As a consequence, we need $\mu = -\sigma^2/2$ to impose $\langle \varepsilon_*/\varepsilon_0 \rangle = \langle f^{1/n} \rangle = 1$. And the previous equation simplifies into

$$\frac{df}{f} = \left(n\tau \frac{d}{dt} \ln \frac{\varepsilon_\Delta}{\varepsilon_0} - \ln \left[\left(\frac{\varepsilon_0}{\varepsilon_\Delta} \right)^n f \right] + n\left(n - \frac{1}{2} \right) \sigma^2 \right) \frac{dt}{\tau} + \sqrt{\frac{2n^2\sigma^2}{\tau}} dW$$

or

$$\frac{d\varepsilon_*^n}{\varepsilon_*^n} = \left(n\tau \frac{d}{dt} \ln \frac{\varepsilon_\Delta}{\varepsilon_0} - \ln \frac{\varepsilon_*^n}{\varepsilon_\Delta^n} + n\left(n - \frac{1}{2} \right) \sigma^2 \right) \frac{dt}{\tau} + \sqrt{\frac{2n^2\sigma^2}{\tau}} dW.$$

APPENDIX B: STOCHASTIC PROCESS ON THE SURFACE OF A SPHERE

In the orientation process, the vector $\mathbf{e}_*$ is modified by a random increment:

$$\mathbf{e}_*(t + dt) = \mathbf{e}_*(t) + d\mathbf{e}_*(t). \tag{B1}$$

To satisfy the normalization constraint at all times,

$$|\mathbf{e}_*(t + dt)| = |\mathbf{e}_*(t)| = 1, \tag{B2}$$

we introduced the following projection:

$$\mathbf{e}_*(t + dt) = \frac{\mathbf{e}_\diamond(t + dt)}{|\mathbf{e}_\diamond(t + dt)|}, \tag{B3}$$

where $\mathbf{e}_\diamond(t + dt)$ represents the predicted orientation vector which is obtained from

$$\mathbf{e}_\diamond(t + dt) = \mathbf{e}_*(t) + d\mathbf{e}_\diamond(t). \tag{B4}$$

The predictor increment process $d\mathbf{e}_\diamond(t)$ is given later. Taking the notation $\gamma = |\mathbf{e}_\diamond(t + dt)|^{-1}$ and substituting Eq. (B4) into Eq. (B3) gives

$$\mathbf{e}_*(t + dt) = \gamma \left[\mathbf{e}_*(t) + d\mathbf{e}_\diamond(t) \right], \tag{B5}$$

and reporting into Eq. (B1) yields the increment of the orientation vector satisfying the normalization constraint:

$$d\mathbf{e}_*(t) = (\gamma - 1)\mathbf{e}_*(t) + \gamma d\mathbf{e}_\diamond(t). \tag{B6}$$

Concerning the prediction for the orientation increment $d\mathbf{e}_\diamond(t)$ it is obtained by an angular displacement of a point on the surface of the sphere moving with the angular velocity $\boldsymbol{\alpha}$ during a time interval dt:

$$d\mathbf{e}_\diamond(t) = \mathbf{e}_*(t) \times \boldsymbol{\alpha} dt. \tag{B7}$$

Substituting this relation into Eq. (B4) one can express $\gamma = |\mathbf{e}_\diamond(t+dt)|^{-1}$ as

$$\begin{aligned}\gamma &= \left[\underbrace{\mathbf{e}_*(t)^2}_{=1} + d\mathbf{e}_\diamond(t)^2 + 2\mathbf{e}_*(t) \cdot d\mathbf{e}_\diamond(t) \right]^{-1/2} \\ &= \left[1 + (\mathbf{e}_*(t) \times \boldsymbol{\alpha} dt)^2 + 2 \underbrace{\mathbf{e}_*(t) \cdot (\mathbf{e}_*(t) \times \boldsymbol{\alpha} dt)}_{=0} \right]^{-1/2} \\ &= \left[1 + \underbrace{\mathbf{e}_*(t)^2}_{=1} \boldsymbol{\alpha}^2 dt^2 - (\mathbf{e}_*(t) \cdot \boldsymbol{\alpha} dt)^2 \right]^{-1/2}. \end{aligned} \tag{B8}$$

As specified in Eq. (15), the angular velocity $\boldsymbol{\alpha}$ evolves according to an Ornstein-Uhlenbeck process.

[1] C. Meneveau and J. Katz, Scale-invariance and turbulence models for large-eddy simulation, Annu. Rev. Fluid Mech. **32**, 1 (2000).

[2] P. Sagaut, *Large Eddy Simulation for Incompressible Flows: An introduction*, 2nd ed. (Springer Verlag, Berlin, 2002).

[3] R. Gatignol, The Faxén formulae for a rigid particle in an unsteady nonuniform Stokes flow, J. Mec. Theor. Appl. **1**, 143 (1983).

[4] M. R. Maxey and J. J. Riley, Equation of motion for a small rigid sphere in a nonuniform flow, Phys. Fluids **26**, 883 (1983).

[5] G. A. Voth, A. La Porta, A. M. Grawford, J. Alexander, and E. Bodenschatz, Measurements of particle accelerations in fully developed turbulence, J. Fluid Mech. **469**, 121 (2002).

[6] N. Mordant, J. Delour, E. Léveque, O. Michel, A. Arnéodo, and J.-F. Pinton, Lagrangian velocity fluctuations in fully developed turbulence: Scaling, intermittency, and dynamics, J. Stat. Phys. **113**, 701 (2003).

[7] S. Ayyalasomayajula, A. Gylfason, L. R. Collins, E. Bodenschatz, and Z. Warhaft, Lagrangian Measurements of Inertial Particle Accelerations in Grid-Generated Wind Tunnel Turbulence, Phys. Rev. Lett. **97**, 144507 (2006).

[8] N. M. Qureshi, M. Bourgoin, C. Baudet, A. Cartellier, and Y. Gagne, Turbulent Tranport of Materials Particles: An Experimental Investigation of Finite-Size Effect, Phys. Rev. Lett. **99**, 184502 (2007).

[9] R. Volk, E. Calzavarini, G. Verhille, D. Lohse, N. Mordant, J.-F. Pinton, and F. Toschi, Acceleration of heavy and light particles in turbulence: Comparison between experiments and direct numerical simulations, Physica D: Nonlin. Phenom. **237**, 2084 (2008).

[10] H. Xu and E. Bodenschatz, Motion of inertial particles with size larger than kolmogorov scale in turbulent flows, Physica D: Nonlin. Phenom. **237**, 2095 (2008).

[11] N. M. Qureshi, U. Arrieta, C. Baudet, A. Cartellier, Y. Gagne, and M. Bourgoin, Acceleration statistics of inertial particles in turbulent flow, Eur. Phys. J. B **66**, 531 (2008).

[12] J. C. Vassilicos, Dissipation in turbulent flows, Annu. Rev. Fluid Mech. **47**, 95 (2015).

[13] F. Toschi and E. Bodenschatz, Lagrangian properties of particles in turbulence, Annu. Rev. Fluid Mech. **41**, 375 (2009).
[14] B. Castaing, Y. Gagne, and E. J. Hopfinger, Velocity probability density functions of high Reynolds number turbulence, Physica D: Nonlin. Phenom. **46**, 177 (1990).
[15] P. K. Yeung, S. B. Pope, A. G. Lamorgese, and D. A. Donzis, Acceleration and dissipation statistics of numerically simulated isotropic turbulence, Phys. Fluids **18**, 065103 (2006).
[16] P. Fede and O. Simonin, Numerical study of the subgrid fluid turbulence effects on the statistics of heavy colliding particles, Phys. Fluids **18**, 045103 (2006).
[17] V. R. Kuznetsov and V. A. Sabel'nikov, *Turbulence and Combustion* (Hemisphere Publishing Corporation, Washington, DC, 1990).
[18] A. A. Shraiber, L. B. Gavin, V. A. Naumov, and o V. P. Yatsenk, *Hydromechanics of Two-component Flows with Polydisperse Material* (Naukova Dumka, Kiev, 1980).
[19] H. Tennekes and J. L. Lumley, *A First Course in Turbulence* (MIT Press, Cambridge, MA, 1972).
[20] M. Bourgoin, N. M. N. M. Qureshi, C. Baudet, A. Cartellier, and Y. Gagne, Turbulent transport of finite sized material particles, J. Phys.: Conference Series **318**, 012005 (2011).
[21] R. Volk, E. Calzavarini, E. Lévêque, and J.-F. Pinton, Dynamics of inertial particles in a turbulent von kármán flow, J. Fluid Mech. **668**, 223 (2011).
[22] E. Calzavarini, R. Volk, M. Bourgoin, E. Lévêque, J.-F. Pinton, and F. Toschi, Acceleration statistics of finite-sized particles in turbulent flow: The role of faxén forces, J. Fluid Mech. **630**, 179 (2009).
[23] E. Loth and A. J. Dorgan, An equation of motion for particles of finite Reynolds number and size, Environ. Fluid Mech. **9**, 187 (2009).
[24] C. Marchioli, Large-eddy simulation of turbulent dispersed flows: A review of modelling approaches, Acta Mech. **228**, 741 (2017).
[25] B. L. Sawford, Reynolds number effects in Lagrangian stochastic models of turbulent dispersion, Phys. Fluids A **3**, 1577 (1991).
[26] S. B. Pope, Stochastic Lagrangian models of velocity in homogeneous turbulent shear flow, Phys. Fluids **14**, 1696 (2002).
[27] S. B. Pope and Y. L. Chen, The velocity-dissipation probability density function model for turbulent flows, Phys. Fluids **2**, 1437 (1990).
[28] V. Sabel'nikov, A. Chtab-Desportes, and M. Gorokhovski, New sub-grid stochastic acceleration model in LES of high-Reynolds-number flows, Eur. Phys. J. B **80**, 177 (2011).
[29] R. Zamansky, I. Vinkovic, and M. Gorokhovski, Acceleration in turbulent channel flow: Universalities in statistics, subgrid stochastic models and an application, J. Fluid Mech. **721**, 627 (2013).
[30] J. Pozorski and S. V. Apte, Filtered particle tracking in isotropic turbulence and stochastic modeling of subgrid-scale dispersion, Int. J. Multiphase Flow **35**, 118 (2009).
[31] B. J. Geurts and J. G. M. Kuerten, Ideal stochastic forcing for the motion of particles in large-eddy simulation extracted from direct numerical simulation of turbulent channel flow, Phys. Fluids **24**, 081702 (2012).
[32] I. M. Mazzitelli, F. Toschi, and A. S. Lanotte, An accurate and efficient Lagrangian subgrid model, Phys. Fluids **26**, 095101 (2014).
[33] S. Chibbaro, C. Marchioli, M. V. Salvetti, and A. Soldati, Particle tracking in les flow fields: Conditional Lagrangian statistics of filtering error, J. Turbulence **15**, 22 (2014).
[34] A. Innocenti, C. Marchioli, and S. Chibbaro, Lagrangian filtered density function for LES-based stochastic modelling of turbulent particle-laden flows, Phys. Fluids **28**, 115106 (2016).
[35] P. L. Johnson and C. Meneveau, Predicting viscous-range velocity gradient dynamics in large-eddy simulations of turbulence, J. Fluid Mech. **837**, 80 (2017).
[36] G. I. Park, M. Bassenne, J. Urzay, and P. Moin, A simple dynamic subgrid-scale model for LES of particle-laden turbulence, Phys. Rev. Fluids **2** (2017).
[37] J. Bec, L. Biferale, M. Cencini, A. Lanotte, and F. Toschi, Intermittency in the velocity distribution of heavy particles in turbulence, J. Fluid Mech. **646**, 527 (2010).
[38] S. B. Pope, *Turbulent Flows* (Cambridge University Press, Cambridge, 2000).

[39] R. Zamansky, F. Coletti, M. Massot, and A. Mani, Radiation induces turbulence in particle-laden fluids, Phys. Fluids **26**, 071701 (2014).
[40] R. Zamansky, F. Coletti, M. Massot, and A. Mani, Turbulent thermal convection driven by heated inertial particles, J. Fluid Mech. **809**, 390 (2016).
[41] S. Chen, G. D. Doolen, R. H. Kraichnan, and Z. She, On statistical correlations between velocity increments and locally averaged dissipation in homogeneous turbulence, Phys. Fluids A **5**, 458 (1993).
[42] Y. Kaneda, T. Ishihara, M. Yokokawa, K. Itakura, and A. Uno, Energy dissipation rate and energy spectrum in high resolution direct numerical simulations of turbulence in a periodic box, Phys. Fluids **15**, L21 (2003).
[43] P. K. Yeung and S. B. Pope, An algorithm for tracking fluid particles in numerical simulations of homogeneous turbulent, J. Comput. Phys. **79**, 373 (1988).
[44] B. L. Sawford, P. K. Yeung, M. S. Borgas, P. Vedula, A. La Porta, A. M. Crawford, and E. Bodenschatz, Conditional and unconditional acceleration statistics in turbulence, Phys. Fluids **15**, 3478 (2003).
[45] J. Bec, L. Biferale, G. Boffetta, A. Celani, M. Cencini, A. Lanotte, S. Musacchio, and F. Toschi, Acceleration statistics of heavy particles in turbulence, J. Fluid Mech. **550**, 349 (2006).
[46] A. N. Kolmogorov, A refinement of previous hypotheses concerning the local structure of turbulence in a viscous incompressible fluid at high Reynolds number.J. Fluid Mech. **13**, 82 (1962).
[47] A. M. Oboukhov, Some specific features of atmospheric tubulence, J. Fluid Mech. **13**, 77 (1962).
[48] N. Mordant, A. M. Crawford, and E. Bodenschatz, Three-Dimensional Structure of the Lagrangian Acceleration in Turbulent Flows, Phys. Rev. Lett. **93**, 214501 (2004).
[49] S. B. Pope, Lagrangian microscales in turbulence, Philos. Trans. R. Soc. London **333**, 309 (1990).
[50] A. G. Lamorgese, S. B. Pope, P. K. Yeung, and B. L. Sawford, A conditionally cubic-Gaussian stochastic Lagrangian model for acceleration in isotropic turbulence, J. Fluid Mech. **582**, 423 (2007).
[51] M. Wilkinson and A. Pumir, Spherical ornstein-uhlenbeck processes, J. Stat. Phys. **145**, 113 (2011).
[52] Y. P. Kalmykov and W. T. Coffey, *The Langevin Equation With Applications to Stochastic Problems in Physics, Chemistry and Electrical Engineering* (World Scientific, Singapore, 2012).
[53] J. T. Lewis, J. McConnell, and B. K. P. Scaife, The rotational Brownian motion of a sphere, Phys. Lett. A **49**, 303 (1974).
[54] P. Debye, Polar molecules, J. Soc. Chem. Industry **48**, 1036 (1929).
[55] H. Xu, A. Pumir, G. Falkovich, E. Bodenschatz, M. Shats, H. Xia, N. Francois, and G. Boffetta, Flight-crash events in turbulence, Proc. Natl. Acad. Sci. USA **111**, 7558 (2014).
[56] H. Homann and J. Bec, Finite-size effects in the dynamics of neutrally buoyant particles in turbulent flow, J. Fluid Mech. **651**, 81 (2010).
[57] M. Uhlmann and A. Chouippe, Clustering and preferential concentration of finite-size particles in forced homogeneous-isotropic turbulence, J. Fluid Mech. **812**, 991 (2017).
[58] R. Clift, J. Grace, and M. Weber, *Bubble, Drops and Particles* (Academic Press, San Diego, CA, 1978).
[59] S. V. Apte, K. Mahesh, and T. Lundgren, Accounting for finite-size effect in disperse two-phase flow, Int. J. Multiphase Flow **34**, 260 (2008).
[60] R. D. Brown, Z. Warhaft, and G. A. Voth, Acceleration Statistics of Neutrally Buoyant Spherical Particles in Intense Turbulence, Phys. Rev. Lett. **103**, 194501 (2009).
[61] T. M. Burton and J. K. Eaton, Fully resolved simulations of particle-turbulence interaction, J. Fluid Mech. **545**, 67 (2005).
[62] A. Naso and A. Prosperetti, The interaction between a solid particle and a turbulent flow, New J. Phys. **12**, 033040 (2010).
[63] H. Homann, J. Bec, and R. Grauer, Effect of turbulent fluctuations on the drag and lift forces on a towed sphere and its boundary layer, J. Fluid Mech. **721**, 155 (2013).
[64] M. Cisse, H. Homann, and J. Bec, Slipping motion of large neutrally buoyant particles in turbulence, J. Fluid Mech. (2013) 735.
[65] R. Zimmermann, Y. Gasteuil, M. Bourgoin, R. Volk, A. Pumir, and J.-F. Pinton, Rotational Intermittency and Turbulence Induced Lift Experienced by Large Particles in a Turbulent Flow, Phys. Rev. Lett. **106**, 154501 (2011).
[66] International CFD Database, https://doi.org/10.4121/uuid:a64319d5-1735-4bf1-944b-8e9187e4b9d6.